Adiabatic transfer for atomic interferometry

Paul D. Featonby, Gilford S. Summy, Jocelyn L. Martin, Huang Wu, Kendrick P. Zetie, Christopher J. Foot, and Keith Burnett

Clarendon Laboratory, Department of Physics, University of Oxford, Parks Road, Oxford OX1 3PU, United Kingdom

(Received 5 July 1995; revised manuscript received 6 September 1995)

We have observed momentum transfer in cesium atoms using the process of adiabatic transfer between dark states. We have investigated the sensitivity of this process to Zeeman shifts and to the differences between the translational energies of the states involved. We have shown that, for a chosen velocity class, the resultant phase shifts of the magnetic substates can be canceled so a dark state is maintained. Two different laser polarization configurations were used to perform the experiments: two circularly polarized beams or a linearly and a circularly polarized beam. Results for each are presented. Finally we discuss the relevance of our results to atomic interferometry and consider methods to minimize the possible phase shifts introduced in an atomic interferometer based upon adiabatic transfer.

PACS number(s): 42.50.Vk, 03.75.Dg, 07.60.Ly

I. INTRODUCTION

The manipulation of atoms with light is now a well established field. Optical forces have been employed in many applications ranging from cooling and trapping [1] to atom interferometry [2]. One recent development has been the technique of momentum transfer with adiabatic passage using delayed laser pulses [3]. Adiabatic transfer has its origins in nuclear magnetic resonance studies in which adiabatic passage was used to change the nuclear magnetization [4]. The process can also be performed in the optical domain with copropagating laser beams of different polarizations or frequencies. This technique was first used for molecular population transfer [5] before being applied to the transfer of population between the magnetic sublevels of an atomic system [6].

In addition to transferring populations, if the laser beams are propagating in different directions, adiabatic transfer will involve a change in the momentum of the system. In this situation the internal states of the atom are associated with particular values of momentum, so that any change of atomic state has a corresponding change in momentum. This has been demonstrated between the different magnetic sublevels of the cesium ground state using delayed pulses of counterpropagating σ^+ and σ^- polarized light [3]. Similar experiments in metastable helium [7] have additionally shown the feasibility of using orthogonal linearly polarized laser beams traveling in opposite directions to deflect an atomic beam.

Because of its ability to change momentum and population, adiabatic transfer was proposed as a means of realizing coherent mirrors and beam splitters for atoms [8]. It has significant advantages over Raman techniques [2], as it is relatively insensitive to the laser intensity and pulse length and the atomic coherence is still, in principle, preserved. During an ideal adiabatic transfer the atoms remain in a state with zero transition amplitude to an excited state, a so-called ''dark'' state. This ensures that there is no population in the excited state, so that spontaneous emission is inhibited.

The coherent nature of adiabatic transfer makes it an excellent tool for the manipulation of atomic wave packets for interferometry [9]. By performing a transfer partially, so that the final state is a superposition state with a variety of momenta, the process may be used as an atomic beam splitter [7]. When a complete transfer is carried out, the final state has a discrete momentum and the process can be used as a ''mirror.'' With these ''optical elements'' atomic wave packets may be split and recombined to construct an interferometer.

In this paper we begin by discussing the theory of adiabatic transfer, before considering how different phase shifts introduced during the process may be canceled. We also consider velocity selection during adiabatic transfer, explaining why it occurs and how the velocities selected by the process can be changed using magnetic fields. We present results confirming the theory and finally discuss our results in the context of atomic interferometry and the minimization of phase shifts accumulated by the atomic wave packet. In particular we discuss the use of a $\sigma^+\pi$ light configuration to perform adiabatic transfer, as this can lead to reduced magnetic-field sensitivity, an important factor in the design of atomic interferometers.

II. ADIABATIC TRANSFER: THEORY

We begin by considering the example of an $F=1$ to $F'=1$ transition interacting with linearly (π) and circularly polarized (σ^+) light to explain the principle of adiabatic transfer. The z axis is defined as the quantization axis and the direction of propagation of the circularly polarized beam. To preserve the usual selection rules the linearly polarized beam must propagate in the x-y plane with its electric field vector in the z direction. For convenience we choose the propagation of the linear beam to be along the x axis.

The light field interaction Hamiltonian is

$$V=\frac{\hbar\Omega_1(t)}{2}e^{i(\omega t-kz)}[|e_0\rangle\langle g_{-1}|+|e_{+1}\rangle\langle g_0|]+\frac{\hbar\Omega_2(t)}{2}e^{i(\omega t-kx)+i\phi}[|e_{-1}\rangle\langle g_{-1}|+|e_{+1}\rangle\langle g_{+1}|]+\text{H.c.}, \quad (1)$$

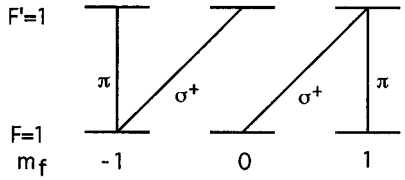

FIG. 1. Allowed transitions with σ^+ and π light of an $F=1$ to $F'=1$ transition.

where we have not included the momentum labels for the states. $\Omega_1(t)$ and $\Omega_2(t)$ are the Rabi frequencies of the circularly and linearly polarized beams, respectively, and ϕ is the phase difference between the two light beams. These transitions are shown in Fig. 1.

Dark states $|\psi_d\rangle$ are by definition a superposition of the ground states that must satisfy $V|\psi_d\rangle=0$. In this example the dark state is found to be

$$|\psi_d\rangle=\frac{1}{\Omega(t)}[\Omega_2(t)|g_0\rangle-e^{-i\phi}\Omega_1(t)|g_{+1}\rangle], \tag{2}$$

$\Omega(t)=(\Omega_1^2(t)+\Omega_2^2(t))^{1/2}$ being a normalizing factor.

From this analysis it can be seen that the exact composition of the dark state depends upon the intensities of the laser beams via the Rabi frequencies $\Omega_1(t)$ and $\Omega_2(t)$. If the intensities are changed slowly enough such that the adiabatic condition is fulfilled, then an atom is kept in a dark state while this state changes from one ground-state superposition to another. Thus, atoms initially in the $m_f=0$ state can be transferred to the $m_f=+1$ state while remaining dark.

The generalized adiabatic condition requires that the Rabi frequencies change slowly enough so that the atomic system may follow the dark state. That is,

$$\Omega T\gg 1 \quad \text{for} \quad \Omega\gg\Gamma, \tag{3a}$$

$$\Omega^2 T\gg\Gamma \quad \text{for} \quad \Omega\ll\Gamma, \tag{3b}$$

where T is the pulse length used for the adiabatic transfer and Γ is the decay rate of the excited state. If the Rabi frequency and pulse length do not satisfy these conditions, then an additional coupling is introduced that causes a mixing between the dark and excited state [10].

In the analysis so far it has been assumed that the substates of the ground level are degenerate with each other. If this is not the case, then an additional phase factor that changes linearly with time must be attached to each substate. For constant Ω_1 and Ω_2 the dark state will evolve to a new superposition given by

$$|\psi\rangle=\frac{1}{\Omega}[\Omega_2 e^{iE_{g_0}t/\hbar}|g_0\rangle-e^{-i\phi}\Omega_1 e^{iE_{g_{+1}}t/\hbar}|g_{+1}\rangle]. \tag{4}$$

We can calculate the overlap between the dark state given by Eq. (2) and the actual state of Eq. (4). This is

$$|\langle\psi_d|\psi\rangle|^2=\frac{1}{\Omega^4}[\Omega_1^4+\Omega_2^4+2\Omega_1^2\Omega_2^2\cos(\Delta Et/2\hbar)], \tag{5}$$

where $\Delta E=E_{g_0}-E_{g_{+1}}$.

Clearly $|\psi\rangle$ will only be completely dark when the argument of the cosine is zero or some integral multiple of 2π, so that $|\langle\psi_d|\psi\rangle|^2=1$. Hence for $|\psi\rangle$ to be dark at all times we require $\Delta E=0$.

Because we used the cesium $6\,^2S_{1/2}(F=4)-6\,^2P_{3/2}(F'=4)$ transition in our experiment, we now turn to consider adiabatic transfer in an $F=4$ to $F'=4$ system. In this case the theory is more complicated due to the ninefold degeneracy of the ground state, although it is still possible to use a reasonably simple model to understand the processes.

It can be seen that atoms that populate the $F=4,m_f=0$ state, which are irradiated with linearly polarized light, must be dark, since

$$\langle F=4,m_f=0|V(\Omega_1=0,\Omega_2=\Omega)|F'=4,m_f=0\rangle=0. \tag{6}$$

Similarly, atoms in the $m_f=+4$ state, which are exposed to σ^+ circularly polarized light, must also be dark because with this polarization there are no allowed transitions from this state. Thus, a situation can be envisaged where atoms begin in the $m_f=0$ state in the presence of π polarized light and slowly evolve to the $m_f=+4$ state as the intensity of the π polarization is reduced and replaced with light from a σ^+ polarized beam. This is indicated in Fig. 2.

The amount of momentum that is imparted during an adiabatic transfer can be related to the number of stimulated emissions and absorptions that would occur if the atom moved between the states in stimulated single-photon processes. Thus, an atom moving from $m_f=0$ to $m_f=+4$ in the ground state can be considered to absorb four σ^+ photons and emit four π photons. It should be emphasized that in a perfect adiabatic transfer the excited-state population is always zero, and thus there can be no spontaneous emission. The directions of the light beams are required to be such that the linearly polarized light is perpendicular to the circularly polarized light. It follows that the total momentum change is $4\sqrt{2}\hbar k$, in a direction at 45° to each of the beams.

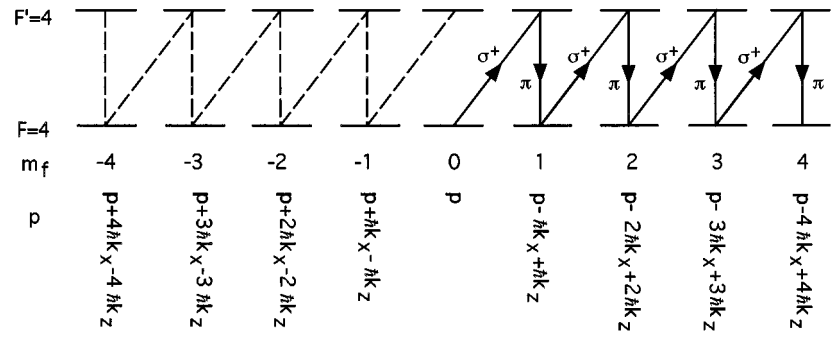

FIG. 2. Evolution of atoms in the dark state from $m_f=0$ to $m_f=+4$ as the intensity of the σ^+ and π light is changed. The arrows indicate the direction of transfer and the dotted lines represent transitions that are not used. The momentum associated with each state is also listed.

Because cesium has two ground states, any atoms that do not undergo adiabatic transfer in the $F=4$ ground state and are lost from the dark state will be optically pumped to the $F=3$ state.

III. CANCELLATION OF PHASE SHIFTS

Adiabatic transfer with optical pulses of identical frequency between different m_f states will be most efficient when the states involved in the process are degenerate. If this is not the case, then a phase shift will be introduced between the levels and this will tend to destroy the dark state. We see from Eq. (4) that an energy difference between m_f states will lead to a less efficient transfer because the superposition state is not perfectly dark. Clearly the Zeeman shift will introduce such an energy difference. It has therefore been suggested [2], that this shift makes it inappropriate to use such magnetically sensitive systems for precision experiments. However, one must also take into account the kinetic energy differences or Doppler shifts that occur between the m_f states that comprise the dark state. As both Zeeman shift and Doppler shift are to first order proportional to m_f, it is possible to cancel one term with the other through the appropriate choice of velocity and magnetic field. This means that adiabatic transfer will be accompanied by selection of velocity, the value depending upon the magnetic field applied. We shall now describe in detail the nature of this velocity selection.

A. The $\sigma^+\sigma^-$ configuration

In addition to the $\sigma^+\pi$ configuration we have discussed, the use of two counterpropagating beams of opposite circular polarization to perform adiabatic transfer has been demonstrated [3]. With this $\sigma^+\sigma^-$ beam arrangement we can calculate the kinetic and magnetic energies of two adjacent m_f states of the dark state. The energy differences between the m_f and m_f-2 states are

$$\Delta E_{\mathrm{KE}}(m_f)=\frac{[p_z+m_f\hbar k]^2}{2m}-\frac{[p_z+(m_f-2)\hbar k]^2}{2m},$$

$$=\frac{2\hbar k p_z}{m}+\frac{2(m_f-1)(\hbar k)^2}{m}, \tag{7}$$

$$\Delta E_{\mathrm{ME}}(m_f)=2g_f\mu_B B. \tag{8}$$

In order to minimize the energy differences between the m_f states we require

$$\Delta E_{\mathrm{KE}}(m_f)+\Delta E_{\mathrm{ME}}(m_f)=0; \tag{9}$$

that is,

$$p_z=-\frac{mg_f\mu_B}{\hbar k}B-\frac{(m_f-1)\hbar k}{2}. \tag{10}$$

Since this equation depends upon m_f, for a level with $F>1$ it is impossible for all magnetic substates to satisfy it simultaneously [11]. This implies that for a state composed of different magnetic substates there is no superposition that is completely dark when $F>1$. In other words, for this situation every superposition of magnetic substates must have an intrinsic leakiness associated with it.

B. The $\sigma^+\pi$ configuration

A similar analysis may be performed for the $\sigma^+\pi$ polarization configuration, where it can be shown that the magnetic energy and kinetic energy phase shifts can be partially canceled. The kinetic energy is given by

$$E_{\mathrm{KE}}(m_f)=\frac{1}{2m}[(p_x-m_f\hbar k)^2+p_y^2+(p_z+m_f\hbar k)^2]. \tag{11}$$

We consider the kinetic energy difference between two adjacent m_f states of the dark state. This energy difference between the m_f and m_f-1 states is

$$\Delta E_{\mathrm{KE}}(m_f)=\frac{1}{2m}[2(p_z-p_x)\hbar k-2\hbar^2(2m_f-1)k^2]. \tag{12}$$

Comparing this with the Zeeman term we find the condition

$$\mu_B g_f B=-\frac{\hbar k}{m}(p_z-p_x)-\frac{(2m_f-1)\hbar^2k^2}{m}, \tag{13}$$

$$p_z-p_x=-\frac{m\mu_B g_f}{\hbar k}B-(2m_f-1)\hbar k, \tag{14}$$

in order to cancel the energy differences between the different m_f states. We discuss the significance of this equation in the following section. Similar to the $\sigma^+\sigma^-$ configuration, there is a term arising from the kinetic energy that cannot be canceled for all m_f states. This again implies that there will be an intrinsic leakiness for any dark superposition state that is formed from a level with $F>1$.

The two schemes presented here are very similar in terms of the energy differences introduced and their cancellation. Both configurations have an intrinsic leakiness of a similar size associated with them.

IV. VELOCITY SELECTION DURING ADIABATIC TRANSFER

It has been seen in Sec. III that atomic kinetic energies can break the degeneracy of the m_f levels, making adiabatic transfer inefficient if an appropriate magnetic field is absent. For a given magnetic field only atoms of a certain velocity will undergo adiabatic transfer. Naturally there is a finite probability of atoms with velocities around this value being transferred. This leads to a width of the dark state in momentum space that is approximately proportional to the square root of the inverse pulse length [12]. For the $\sigma^+\sigma^-$ case the momentum selection is in the direction of the two circularly polarized beams; that is, along the z axis. By looking at the atomic momentum in this direction it should be possible to see a change in the momentum width of the atoms that are transferred as the pulse length is varied. For the $\sigma^+\pi$ case, Eq. (14) shows that only atoms whose momentum satisfies $p_z-p_x=c$, where $c=-m\mu_B g_f B/\hbar k$, will be selected. In obtaining this equation we have neglected the last term of Eq. (14). This is justified on the grounds that the only effect of this term is to preclude the existence of a perfectly dark

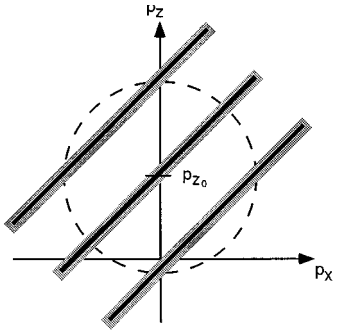

FIG. 3. Momentum space representation of the thermal distribution of atoms before adiabatic transfer (dotted circle). The atoms have been allowed to fall and obtain an average momentum of $p_z = p_{z_0}$. The dark-state momenta for a $\sigma^+\pi$ light configuration are depicted by the lines passing through the circle. Each line represents the dark state for a particular value of the magnetic field in the z direction, while the thickness of the lines indicates the dark-state momentum width.

state. In other words we are considering a line in momentum space of maximum darkness.

The momentum selection will be most easily observed at 45° to both light beams; that is, in a direction perpendicular to the line of maximum darkness. Changes in the momentum distribution will be more difficult to analyze if the momentum can only be resolved along either the x or the z axis. Figure 3 illustrates how the magnetic field selects out the atoms that can exist in a dark state. A circle is used to represent the Gaussian thermal distribution of atoms in momentum space, while the solid lines indicate atoms that will be dark for particular values of the magnetic field. The problem is complicated by the width of the thermal momentum distribution, represented by the radius of the circle, being a function of magnetic field [13]. For simplicity we assume that the probability of an atom being dark is a Gaussian function that depends upon how far the momentum of the atom is from the line of maximum darkness. This concept is illustrated in Fig. 3 by the shadings around each line.

We take the thermal velocity distribution to be

$$T(p_x, p_z) = A e^{-w_T(p_x^2 + (p_z - p_{z_0})^2)}, \tag{15}$$

where $w_T = 1/W^2_{thermal\ width}$, A is a normalizing constant, p_x and p_z are the momenta of the atoms in the x and z directions, and p_{z_0} is the mean momentum of the atoms.

As mentioned above, the dark-state probability in momentum space is represented by a Gaussian function. Although the real distribution is not this simple, it is a good approximation and allows us to write the dark state as

$$D(p_x, p_z) = A' e^{-w_D l^2}, \tag{16}$$

where $w_D = 1/W^2_{dark\text{-}state\ width}$, A' is a normalizing constant, and l represents the distance in momentum space of the atomic momentum from that of maximum darkness. When the line of most darkness satisfies $p_z = p_x + c$ it can be shown that

$$l = \frac{1}{\sqrt{2}}(p_z - p_x - c). \tag{17}$$

By integrating the product of the thermal distribution and the probability of the atom being in the dark state with respect to p_x, we may calculate the momentum distribution of atoms in the dark state along the z axis. It is straightforward to show that the result of this calculation is a Gaussian momentum distribution centered at

$$p_z = \frac{w_D w_T p_{z_0} + (2w_D^2 + w_D w_T)c}{2(w_D^2 + w_D w_T)}. \tag{18}$$

In general this equation depends upon the applied magnetic field in two ways: first through the value of c and second through the initial width of the atomic distribution $W_{thermal\ width}$, which varies approximately quadratically with magnetic field [13]. In Sec. VI we present experimental results that support the theoretical analysis we have given.

The velocity-selective nature of the adiabatic transfer seen in this analysis and the results that follow have many potential applications. One possible use where this technique may well be convenient is the selection of horizontal velocities in atomic fountains as an alternative to Raman transitions. The advantage of adiabatic transfer is that for magnetically insensitive transitions it does not require two different frequencies, as in the Raman technique, and light at the frequency of the $F=4$ to $F'=4$ component of the $D2$ line is readily obtained from any cesium laser cooling experiment.

V. EXPERIMENTAL DETAILS

With the exception of the method used for producing the adiabatic transfer pulses, our experimental apparatus was similar to that described by Goldner *et al.* [3]. Cesium atoms from a standard magneto-optical trap (MOT) [14] were cooled in molasses to temperatures of around 5μK. The cooling light was turned off and the atoms were allowed to fall for a known time before light tuned to the frequency between the $F=4$ and $F'=4$ levels in the $D2$ transition ($6\,^2S_{1/2} - 6\,^2P_{3/2}$) was applied to perform the adiabatic transfer. The $F=4$ to $F'=4$ light was obtained from a laser diode, frequency locked to the crossover resonance between the $F=4$ to $F'=4$ and the $F=4$ to $F'=5$ transitions in the saturated absorption spectrum. This light was then detuned down by 125.7 MHz to the frequency of the $F=4$ to $F'=4$ transition by a single pass through an acoustic-optic modulator (AOM). This AOM, used in conjuction with a mechanical shutter, was used as a switch to turn the light on and off.

The two light pulses required for the adiabatic transfer were produced using an electro-optic modulator (EOM). This device was used as a variable waveplate. The polarization of the incident light could be changed from vertical linear through circular and finally to horizontal linear, by altering the voltage applied to its terminals. A polarizing beam splitter cube placed after the EOM enabled the light to be split into the horizontally and vertically polarized components. A diagram of the apparatus is shown in Fig. 4(a). The intensity of the two beams was directly related to the voltage across

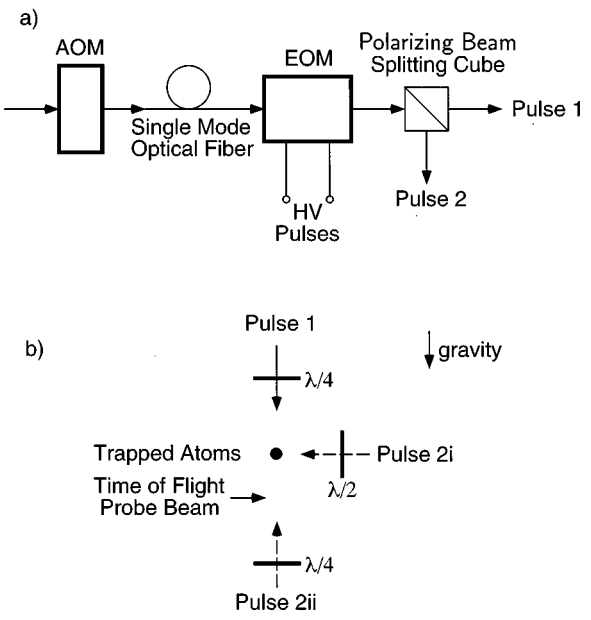

FIG. 4. Experimental configuration used to perform the experiment. The apparatus used to produce the light pulses is shown in (a). The geometry of the laser beams producing the light pulses can be seen in (b). Pulse 2 is either pulse 2i for the $\sigma^+\pi$ configuration or pulse 2ii for the $\sigma^+\sigma^-$ configuration. When linear light was used (pulse 2i) the polarization was in the vertical direction.

the EOM because of the dependence of the phase retardation on the voltage. Thus, by ramping the voltage at the appropriate rate, the intensity in each beam was changed so that the requirements necessary to perform adiabatic transfer could be met. Used in conjunction with the AOM and shutter, the appropriate light pulses were produced, an example of which is shown in Fig. 5(a). Where these pulses were recombined in the interaction region, it was possible to think of the resulting light field as one whose intensity remained constant, but whose overall polarization and direction of propagation changed.

The linear voltage ramp that was used in our experiments led to intensity changes proportional to $\frac{1}{2}(1-\cos t)$ in one beam and $\frac{1}{2}(1+\cos t)$ in the other beam. Hence the Rabi frequency in each of the beams changed, as shown in Fig. 5(b). The length and peak Rabi frequency of these pulses were chosen such that they satisfied the adiabatic conditions given in Eqs. (3a) and (3b). Various pulse lengths were used for the adiabatic transfer, but typically, pulses were 40μs long with a peak power of about 2 mW, corresponding to $\Omega\sim\Gamma$, where Γ is the decay rate of the excited state.

As was the case in the previous theoretical discussion, two different polarization configurations were used. The first consisted of a σ^+ beam propagating downwards and a σ^- beam upwards. The second used a π beam polarized in the vertical direction propagating in a horizontal plane and a σ^+ beam traveling downwards. The geometry of these beams is indicated in Fig. 4(b).

In all experiments we used a time-of-flight (TOF) probe to detect the momentum distribution of the atoms. This consisted of light tuned to the $F=4$ to $F'=5$ transition of the $D2$ line, located approximately 50 cm below the trap. It detected the atoms by looking for fluorescence that was produced as they passed through the beam. From this signal the momentum width of the atoms and also the velocity change that occurred as a result of an adiabatic transfer could be deduced. The light only interacted with atoms in the $F=4$ state because any atoms lost from the dark state were optically pumped to the $F=3$ state during the transfer and were not detected.

The time for which the atoms fell before the adiabatic transfer was performed was varied for different experiments in order to verify that the phase shifts due to the increased kinetic energy could be canceled. This time was of the order of a millisecond.

The earth's magnetic field was canceled in the interaction region by a set of three orthogonal pairs of coils. These were also used to apply a bias field in the vertical direction.

VI. RESULTS

We now present experimental results obtained to confirm the theory presented in the previous sections. Experiments to show the cancellation of the Zeeman shift and the Doppler shift were performed with both the $\sigma^+\sigma^-$ and the $\sigma^+\pi$ configurations.

From Eq. (10), we expect when using $\sigma^+\sigma^-$ pulses that a plot of magnetic field against the momentum of the atoms in the dark state will produce a straight line with the gradient $-m\mu_B g_f/\hbar k$. For a given delay, τ, between cooling and the adiabatic transfer, the centre of the atomic momentum distribution is shifted by an amount $p_{z_0}=mg\tau$. This extra momentum will change the intercept of a plot of magnetic field against momentum while leaving the gradient of the line unchanged.

Carrying out the transfer at different magnetic fields and measuring the resultant change in the momentum of the atoms from the time-of-flight signal, allowed the results shown in Fig. 6 to be obtained. The two sets of data represent different values for τ, the delay before the start of a transfer. As

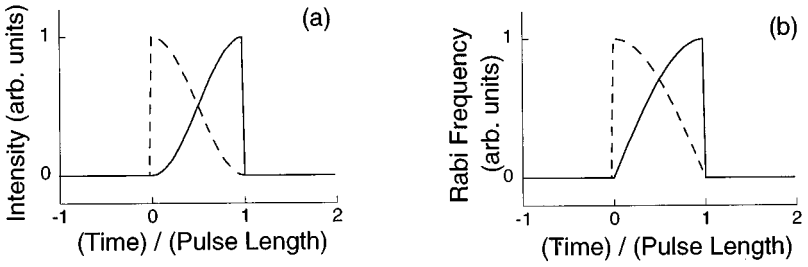

FIG. 5. Variations of the intensity (a) and Rabi frequency (b) in the adiabatic transfer pulse as a function of time. The dotted and solid lines refer to the two different beams used in the pulse.

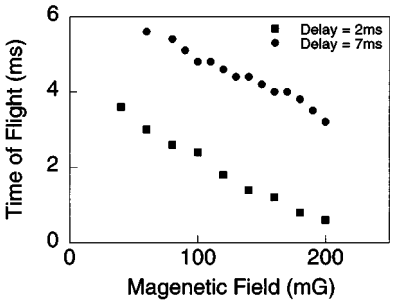

FIG. 6. Change in the time of flight of the atoms as a function of applied magnetic field when a $\sigma^+\sigma^-$ light configuration adiabatic transfer was used. The two sets of data points represent different values of τ, the time between dropping the atoms from the trap and the beginning of the adiabatic transfer.

expected from Eq. (10), a linear variation of the TOF with magnetic field was found. This indicates that the transfer process selected out the velocity class of atoms required in order to make the nondegeneracy of the m_f levels a minimum.

For significant dark-state momentum widths (small pulse lengths) we expect the velocity selection from within the thermal distribution to be less apparent. If one considers a dark-state width much larger than the thermal velocity distribution of the atoms, then it is clear that there will be no apparent velocity selection because all of the atoms can undergo adiabatic transfer in a dark state. For decreasing pulse lengths one would therefore expect the magnitude of the velocity selection to decrease and hence the gradient of the TOF signal as a function of magnetic field to reduce. For long pulse lengths we expect the gradient to tend towards $(-m\mu_B g_f/\hbar k)/mg = -0.03$ ms/mG. Results showing the change in gradient confirm this discussion and are presented in Fig. 7.

We also measured the width of the final momentum distribution, or dark-state width, as a function of pulse length. Typical results are shown in Fig. 8. As the pulse length is increased we expect the momentum width of the transferred atoms to decrease as the dark-state width reduces in size. Qualitatively the reason for the decrease can be considered to be that for longer pulse lengths, phase differences that accumulate between the m_f states due to their different momenta are greater, leading to an increased probability that these atoms leave the dark state. The underlying principle is very similar to that of velocity-selective coherent population trapping, which predicts a momentum width given by $\Delta p \propto 1/\sqrt{T}$, where T is the pulse length used for the adiabatic transfer [12].

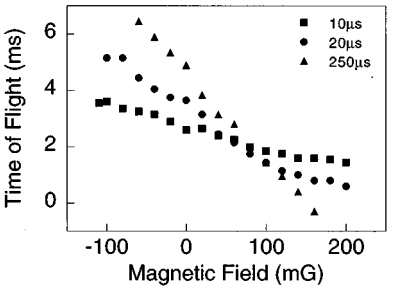

FIG. 7. Change in the time of flight of the atoms as a function of applied magnetic field. The three sets of data points were taken with a $\sigma^+\sigma^-$ light configuration adiabatic transfer for different pulse lengths.

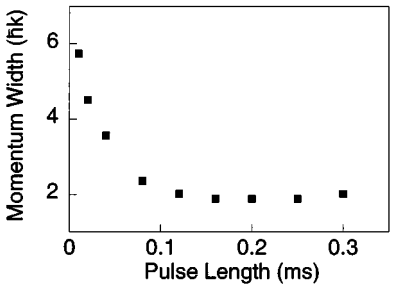

FIG. 8. Momentum width of the transferred atoms as a function of pulse length used to perform the adiabatic transfer. The asymptotic behavior of the width occurs due to the leakiness of the dark state.

It can be seen in Fig. 8 that the momentum width tends to a finite limit as the pulse length is increased. This is a consequence of the leakiness of the dark state in an $F=4$ level. The term in m_f in Eqs. (10) and (14) leads to a range of momenta that are equally dark, and this results in a finite width of the dark state. The off-resonant interactions with other excited hyperfine levels also leads to a finite loss rate from the dark state, which will add to the dark state width. In contrast, for the ideal $F=1$ to $F'=1$ transition of Ref. [14], the temperature will tend to zero with increasing pulse length, as this transition does have a perfect dark state.

Although more difficult to analyze, experiments examining the dependence of the TOF signal on a magnetic field were also carried out for the $\sigma^+\pi$ light configuration. The results obtained are shown in Fig. 9(a). Despite the simple nature of the model used to describe the velocity selection during adiabatic transfer, reasonable agreement is found with the theory from Eq. (18), which is presented in Fig. 9(b).

We can explain the shape of these curves in the following way. For the $\sigma^+\pi$ configuration the dark state contains atoms with a large range of p_z. This can be seen from Fig. 3. This implies that when the thermal width is small, all values of p_z allowed by the thermal distribution may exist in the dark state. Thus, the mean value of p_z will only deviate slightly from the mean vertical momentum of the total atomic distribution. This explains why the gradient of the data given in Fig. 9 is approximately zero for small magnetic fields. As the magnetic field increases, the thermal width becomes considerably larger than the range of vertical momenta that exsist in the dark state. Hence the mean vertical momentum of the atoms in the dark state may be significantly different from the mean vertical momentum of the total atomic distribution. In this situation the gradient becomes independent of the applied magnetic field.

VII. APPLICATIONS TO ATOMIC INTERFEROMETRY

We now consider the relevance of our results to atomic interferometry. Atom interferometers require the atomic wave packet to be split and recombined in a process that preserves the coherence of the atoms. Adiabatic transfer pro-

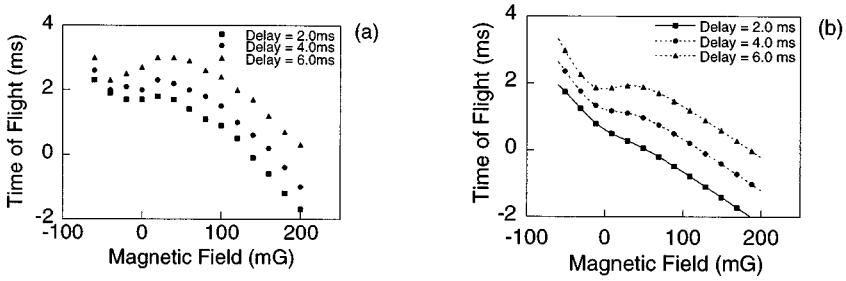

FIG. 9. Change in the time of flight of the atoms as a function of applied magnetic field when $\sigma^+\pi$ adiabatic transfer was used (a). The three sets of experimental data points represent different values of τ, the time between dropping the atoms from the trap and the beginning of the adiabatic transfer. The theoretical data from Eq. (14) for the same three situations is presented in (b).

vides an excellent tool for this if used carefully as spontaneous emission is inhibited and large transfers of momentum are possible. Potential problems mainly concern the susceptibility of adiabatic transfer to unwanted phase shifts from stray magnetic fields and the ac Stark effect.

It has already been seen how sensitive the adiabatic transfer process can be to magnetic fields, where small changes can lead to large effects on the velocity selection within the atomic sample. In an interferometer, unwanted phase shifts may destroy any chance of observing fringes. Thus it is desirable to keep the atoms in a magnetically insensitive $m_f=0$ state for as much of the process as possible. The original $\sigma^+\sigma^-$ transfer technique is not suitable for interferometry because it would require atoms to spend significant lengths of time in magnetically sensitive states. Recently Weitz *et al.* [9] reported on the construction of an atom interferometer using adiabatic transfer with a Raman transition. In this experiment population and momentum were transferred between the $m_f=0$ states of the $F=3$ and $F=4$ ground levels. At all times the atoms remained in states that were insensitive to phase shifts caused by extraneous magnetic fields.

An alternative idea, which is presented here, can be implemented with a single laser frequency, produce larger changes in the momentum of a wave packet, and is less sensitive to other potential problems, such as phase variations in the light pulses. We have seen that adiabatic transfer may be used to move the atomic population between the $m_f=0$ and $m_f=+4$ states using the $\sigma^+\pi$ configuration. However in an interferometer this would lead to unacceptable magnetic-field sensitivity because of the long times between the momentum changing pulses that would have to be spent by the atoms in the magnetically sensitive $m_f=+4$ state. What we therefore propose is to transfer the atoms to the $m_f=+4$ state and then after quickly reversing the beam directions, transfer them back to the $m_f=0$ state. By reversing the directions of the beams the atoms will acquire $8\sqrt{2}\hbar k$ units of momentum rather than the zero momentum that would otherwise result if the beams were kept in the same directions. The pulse sequence to perform this operation is shown in Fig. 10. The main advantage of this scheme is that the atoms are only out of the $m_f=0$ state for the short amount of time required to complete each adiabatic transfer.

Of course other sources of phase shift must also be considered. One of the most significant is that caused by the ac Stark shift from other hyperfine levels in the excited-state manifold. This shift can be minimized in cesium if the $D1$ transition with its large excited-state hyperfine splitting is used. The efficiency of the transfer process for $D1$ light is also much higher because there is less dark state loss caused by off-resonant excitation.

Calculations to assess the efficiency and the size of the phase shifts were performed by integrating the optical Bloch equations during the transfer process. The light pulses that were used were chosen subject to the constraints that the sum of the intensity in the two beams be constant and that the pulse shapes change slowly and smoothly at the beginning and end of a pulse. The latter condition enabled a transfer to be completed using a short pulse length, hence minimizing phase shifts that had a strong time dependence. The Rabi frequencies used in the calculations had the following form:

$$\Omega_1(t)=\Omega_0\cos\left[\frac{\pi}{2}\sin\left(\frac{\pi}{2T}t\right)\right], \tag{19}$$

$$\Omega_2(t)=\Omega_0\sin\left[\frac{\pi}{2}\sin\left(\frac{\pi}{2T}t\right)\right], \tag{20}$$

where Ω_0 is the maximum Rabi frequency.

Figure 11 presents the result of our calculations. The efficiency (a) and phase shifts due to the Zeeman shift and the light shift (b) are plotted for a range of different Rabi frequencies. These results refer to a double pulse, in which the population is transferred from $m_f=0$ to $m_f=+4$ and back again. Note that by choosing the appropriate direction for the magnetic field, the Zeeman shift and light shift can be made to cancel each other. In an experiment in which the pulse length is of the order of 40 μs, and the effective Rabi fre-

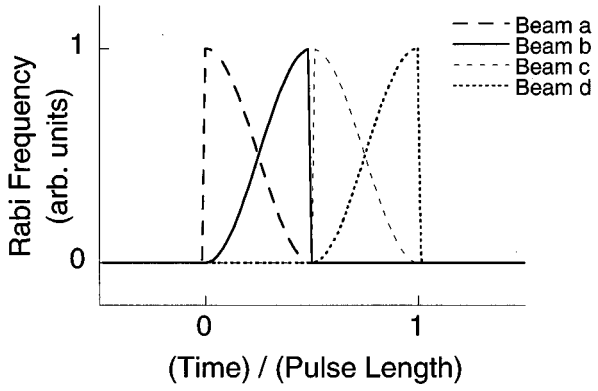

FIG. 10. Adiabatic transfer pulse sequence in which the initial and final configuration of the atoms is the $m_f=0$ state. Beams *a* and *d* are π polarized with opposite directions, beams *b* and *c* are counterpropagating σ^+ polarized beams.

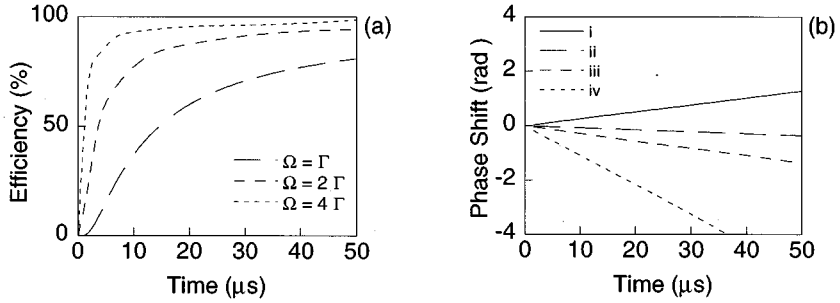

FIG. 11. Efficiencies (a) for adiabatic transfer at different Rabi frequencies using the light pulses of Fig. 10. Phase shifts (b) accumulated during the adiabatic transfer with the same pulse. (i) is the Zeeman shift due to a magnetic field of 10mG, (ii), (iii), and (iv) are the light shifts for Rabi frequencies of Γ, 2Γ, and 4Γ, respectively. The Rabi frequency is defined for a translation with Clebsch-Gordan coefficient of 1. These calculations were performed for the $F=4$ to $F'=4$ transition in the cesium $D1$ line.

quency is around 2Γ, the phase shifts we have calculated are not significant enough to prevent the successful operation of an atomic interferometer.

We believe that the double pulse $\sigma^+\pi$ adiabatic transfer proposed here offers advantages not possessed by other schemes. We are currently involved in the construction of an interferometer based on this concept.

ACKNOWLEDGMENTS

We wish to thank Andrew Wilson for helpful discussions and Chris Townsend for assistance with some of the experiments. This work was supported by an EPSRC grant. H. Wu would like to thank the Sino-British Friendship Scholarship Scheme for support.

[1] J. Opt. Soc. Am. B **6**, 2020 (1989), feature on laser cooling and trapping of atoms, edited by S. Chu and C. Wieman.
[2] M. Kasevich and S. Chu, Phys. Rev. Lett. **67**, 181 (1991).
[3] L. S. Goldner, C. Gerz, R. J. C. Spreeuw, S. L. Rolston, C. I. Westbrook, W. D. Phillips, P. Marte, and P. Zoller, Phys. Rev. Lett. **72**, 997 (1994).
[4] A. Abragam, *The Principles of Nuclear Magnetism* (Clarendon Press, Oxford, 1961).
[5] U. Gaubatz, P. Rudecki, M. Becker, S. Schiemann, M. Külz, and K. Bergmann, Chem. Phys. Lett. **149**, 463 (1988)
[6] P. Pillet, C. Valentin, R. L. Yuan, and J. Yu, Phys. Rev. A **48**, 845 (1993).
[7] J. Lawall and M. Prentiss, Phys. Rev. Lett. **72**, 993 (1994).
[8] P. Marte, P. Zoller, and J. L. Hall, Phys. Rev. A **44**, R4118(1991).
[9] M. Weitz, B. C. Young, and S. Chu, Phys. Rev. Lett. **73**, 2563 (1994).
[10] J. R. Kuklinski, U. Gaubatz, F. T. Hioe, and K. Bergmann, Phys. Rev. A **40**, 6741 (1989).
[11] C. J. Foot, H. Wu, E. Arimondo, and G. Morigi, J. Phys. II France **4**, 1913 (1994).
[12] A. Aspect, E. Arimondo, R. Kaiser, N. Vansteenkiste, and C. Cohen-Tannoudji, Phys. Rev. Lett. **61**, 826 (1988).
[13] P. D. Lett, W. D. Phillips, S. L. Rolston, C. E. Tanner, R. N. Watts, and C. I. Westbrook, J. Opt. Soc. Am. B **6**, 2084 (1989).
[14] E. L. Raab, M. Prentiss, A. Cable, S. Chu, and D. E. Pritchard, Phys. Rev. Lett. **59**, 2631 (1987).